ChemComm
Chemical Communications

Accepted Manuscript

This article can be cited before page numbers have been issued, to do this please use: H. Sun, Y. Qiu, Y. Lu, J. Kong and X. Zhang, *Chem. Commun.*, 2020, DOI: 10.1039/D0CC02176H.

ROYAL SOCIETY OF CHEMISTRY

rsc.li/chemcomm

View Article Online
DOI: 10.1039/D0CC02176H

ChemComm

COMMUNICATION

Ultrasensitive DNA Electrochemical Biosensor Based on MnTBAP Biomimetic Catalyzed AGET ATRP Signal Amplification Reaction

Received 00th January 20xx,
Accepted 00th January 20xx

DOI: 10.1039/x0xx00000x

www.rsc.org/chemcomm

Haobo Sun[a, b†], Yunliang Qiu[c†], Yajie Lu[a], Jinming Kong[b*], Xueji Zhang[d]

In this paper, an ultrasensitive, highly selective and green electrochemical biosensor for quantifying DNA sequences (aM DNA) based on MnTBAP catalyst for AGET ATRP reaction is proposed. For the first time, a combination of biomimetic catalyzed free radical polymerization and DNA electrochemical biosensor was used as a signal amplification strategy.

The early diagnosis of serious diseases such as malignant tumors has always been an important research hotspot.[1-3] Early screening and timely treatment of diseases can significantly improve the survival rate of patients and reduce medical costs. Therefore, detection methods with high sensitivity, high specificity, simple operation, environmental protection and low cost are of great significance in the early diagnosis, observation of efficacy and prognosis monitoring of diseases.[4-6] Gene mutations, including base substitutions and frame shift mutations, can alter the composition or order of amino acids in the encoded polypeptide chain, and then affect the structure and function of proteins or enzymes, leading to the occurrence of diseases. Therefore, it is necessary to carry out early diagnosis of related diseases at the gene level. Compared with traditional deoxyribonucleic acid (DNA) detection methods and analysis, electrochemical DNA biosensor has advantages of low detection cost, simple operation, high sensitivity, easy miniaturization, and broad application prospect in gene detection.[7-10] However, from the perspective of clinical application, the existing electrochemical DNA biosensor analysis methods still have defects such as poor stability and specificity of capture probes, insufficient detection sensitivity, complex preparation process or long detection cycle. Therefore, it is of great significance to improve the stability and specificity of the immobilized capture probe, and to develop a simple, environmental friendly, low-cost and efficient signal amplification strategy, so as to achieve high sensitivity, high selectivity and high-throughput detection of target DNA (T-DNA).

In order to effectively improve the sensitivity and selectivity of electrochemical DNA biosensor analysis and make it suitable for the quantitative analysis of trace T-DNA, it is usually necessary to perform signal amplification on the hybridization reaction between the T-DNA and the capture probe. Signal amplification strategies commonly used in electrochemical DNA biosensor analysis include enzyme catalysis[11,12], target cycling[13,14], polymerase chain reaction (PCR)[15,16], rolling circle amplification (RCA)[17-19], and polymer methods[20-22]. However, most of the them are subject to many limitations. For example, in enzyme-catalyzed signal amplification, natural enzymes have strict requirements on the physical and chemical conditions such as the temperature of the reaction environment. In addition, natural enzymes are usually not cheap and and easily deactivated;[23] In polymer signal amplification, Sun et al reported that electrochemically mediated atom transfer radical polymerization (ATRP) biosensors have potential pollution due to the use of metal catalysts, and this method cannot be used in large quantities due to electrochemical mediation.[24] To overcome these shortcomings, we propose an electrochemical biosensor based on atomic transfer radical polymerization catalyzed by Mn(III) meso-Tetra (4-carboxyphenyl) porphine chloride (MnTBAP) as a model enzyme.

In 1995, the atom transfer radical polymerization reaction developed by Professor Krzysztof Matyjaszewski and Dr. Jinshan Wang achieved real living radical polymerization, which aroused great interest of polymer scientists from all over the world.[25,26] In addition, ATRP has a wide variety of monomers (methacrylate, methacrylamide, styrene, etc.), which can well control the growth length of the polymer chain and synthesize gradient copolymers. And a large number of applications have been made in the fields of material synthesis and surface functionalization. It is therefore suitable for applications in the field of sensing. However, the currently developed biosensors based on living radical polymerization signal amplification have some disadvantages. First, metal catalyst need to be used, which will cause environmental pollution and does not have biocompatibility.[24] Second, electrocatalysis is required through an electrochemical workstation, which makes it impossible to be prepared in large quantities and high throughput.[27] Alternatively, it is necessary to provide additional temperature (> 55 °C), so it can not be operated at room temperature, which will make the operation troublesome.[28]

Metalloporphyrin complexes exist widely in nature and organisms, such as cytochromes, heme, chlorophyll, etc. are metalloporphyrin complexes, which play an important role in life process. Synthetic metalloporphyrins can mimic cytochrome P450, and perform efficient catalytic oxidation of a variety of substrate molecules under mild conditions.[29] In addition, with the development of green

[a] Research Center for Biomedical and Health Science, Anhui Science and Technology University, Fengyang 233100, P. R. China.
[b] School of Environmental and Biological Engineering, Nanjing University of Science and Technology, Nanjing 210094, P. R. China.
[c] Department of Criminal Science and Technology, Nanjing Forest Police College, Nanjing 210023, P. R. China.
[d] School of Biomedical Engineering, Shenzhen University Health Science Center, Shenzhen, Guangdong 518060, P. R. China.
[†]The first two authors are equal first authors.
*Corresponding author. Email: kong@njust.edu.cn
Electronic Supplementary Information (ESI) available.
See DOI: 10.1039/x0xx00000x

chemistry, metalloporphyrin biomimetic catalysis technology has attracted more attention. The technology has the advantages of low price, high economy and no pollution to the environment. Therefore, the synthesis of metalloporphyrins to achieve efficient catalytic oxidation of various organic substrate molecules is a hot topic in recent years. Among them, MnTBAP chloride is a new type of superoxide dismutase (SOD), which has the characteristics of high stability and good cell permeability. In addition, MnTBAP has many advantages as a biomimetic catalyst. First of all, the coordination of the four N atoms in the MnTBAP ring with the Mn ion is very stable. After the Mn ion is coordinated with the N atoms in the porphyrin ring to generate MnTBAP, the Mn ion is difficult to be separated from porphyrin ring in most cases, so the catalytic life of MnTBAP will be increased, and product pollution can be eliminated; Second, MnTBAP does not have active sites for cis coordination. This unique metal coordination can effectively prevent a series of side reactions in the catalytic reaction, so it can improve the catalytic efficiency. Mn porphyrin, as a highly active and selective biomimetic catalyst, has attracted more and more attention.[30,31] Therefore, we provide a method of activators generated by electron transfer atom transfer radical polymerization (AGET ATRP) based on MnTBAP as a model enzyme. This method is environmentally friendly, easy to operate, and can be prepared in large quantities at room temperature. It effectively solves the previous problems of pollution caused by metal catalysis, the need to provide additional temperatures, and the inability to prepare in large quantities. In addition, compared with the signal amplification strategy of directly using of polymers, in-situ growth of polymers can significantly improve the loading capacity of polymer chains and the coupling efficiency on the electrode surface, and solve the problems of insufficient sensitivity and poor selectivity of the existing electrochemical biosensors.

On the basis of the above research work, by virtue of the specific capture characteristics of DNA by PNA and the model enzyme catalyzed AGET ATRP signal amplification, the electrochemical DNA biosensor analysis with high sensitivity, high selectivity, high throughput and environmental friendly detection was carried out. The specific steps of the signal amplification strategy are shown in **Scheme 1A**. Firstly, PNA is covalently bonded to the gold electrode surface by Au-S bond as a capture site for DNA. Then, the interaction between the T-DNA and the PNA allows the PNA probe to capture DNA on the surface of the electrode with high selectivity through the principle of base-pairing, introducing a large amount of phosphate groups. Since the phosphate group also exhibits a strong complex interaction with the zirconium dichloride oxide octahydrate (Zr^{4+}) linkage, and the remaining vacancies of Zr^{4+} can be coordinated to the carboxyl group. Subsequently, the phosphate group in the T-DNA backbone reacts with Zr^{4+}, and the resulting electrode-PNA-T-DNA-Zr^{4+} can bind to the ATRP initiator α-bromophenylacetic acid (BPAA) and the catalyst MnTBAP. Then, a large number of electroactive monomeric ferrocenylmethyl methacrylate (FMMA) were polymerized in situ by MnTBAP catalyzed AGET ATRP onto BPAA to form gold electrode-PNA-T-DNA-Zr^{4+}-$FMMA_n$. As shown in **Scheme 1B**, during this process, Mn^{3+} is first reduced to Mn^{2+} by ascorbic acid (AA), and the initiator R-X (BPAA) reacts with the catalyst Mt^n (Mn^{2+}) to form a free radical R·. The free radical R· reacts with monomer M (FMMA) to form monomer free radical R-M· (R-FMMA·), that is, active R-Mn· (R-$FMMA_n$·) and R-M· (R-FMMA·), which can continue to initiate the free radical polymerization of monomers, and can also take bromine atoms from the dormant species R-M_n-X/ R-M-X to make the free radical disappear and stop the reaction, thereby establishing a reversible equilibrium. That is, a cycle of atomic transfer of bromine atoms from organic bromide to metal complex and metal complex to free radical was constructed, and consequently a large amount of electroactive monomers FMMA were introduced to the electrode surface.(See ESI for the detailed process) Finally, the electroactive polymer ($FMMA_n$) on the electrode surface was used to detect T-DNA quantitatively by enhanced electrochemical signal. This strategy provides new insights into the electrochemical detection of biochemical molecules and has great potential for early screening and diagnosis of different diseases.

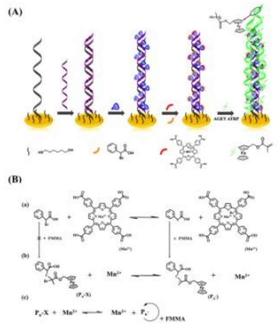

Scheme 1 (A) The schematic diagram showing the preparation process of DNA electrochemical biosensor based on the ATRP signal amplification reaction catalyzed by MnTBAP. (B) Mechanism of ATRP reaction catalyzed by MnTBAP.

To verify the effectiveness of using PNA as a capture probe and the model enzyme-catalyzed AGET ATRP signal amplification strategy, a feasibility analysis of this strategy was performed. The electrode is modified according to the process shown in scheme 1A. In this process, when any of PNA (**Fig. 1A, a**), T-DNA (**Fig. 1A, b**), Zr^{4+} (**Fig. 1A, c**), BPAA (**Fig. 1A, d**), MnTBAP (**Fig. 1A, e**), or FMMA (**Fig. 1A, f**) is not added, the electrochemical signal cannot be obtained. However, when the electrode is modified step by step according to the process shown in **Fig. 1A**, an obvious oxidation peak can be obtained around ~0.33V (**Fig. 1A, g**). The signal is that Fe (II) in FMMA loses an electron on the electrode surface and is oxidized to Fe (III), indicating that FMMA is polymerized to PNA/ T-DNA heteroduplex via AGET ATRP catalyzed by MnTBAP.[24,32] At the same time, the free radicals generated during ATRP have no effect on PNA and DNA.

In order to investigate whether FMMA can be specifically polymerized on the heteroduplex of PNA/ T-DNA, the morphology of the gold electrode surface with or without of T-DNA was observed and monitored by scanning electron microscope (SEM). As shown in **Fig. 1**, when no T-DNA is present (**Fig. 1B**), only polished traces can be seen on the electrode surface, and no polymer formation can be observed. In the presence of T-DNA (**Fig. 1C**), the obtained PNA-T-DNA-Zr^{4+}-BPAA-MnTBAP-$FMMA_n$-modified electrode can be clearly see many obvious island-like protrusions, indicating that a large amount of polymer was formed on the electrode surface. In addition, in order to demonstrate that the observed polymer is adsorbed to the electrode surface through covalent connection rather than non-specific adsorption, the electrode modified by PNA-T-DNA-Zr^{4+}-BPAA-MnTBAP-$FMMA_n$ was electrochemical characterized at different scanning rates using cyclic voltammetry (CV). As shown in **Fig. 1D**, as the scan rate increases, the potential is basically unchanged, and the redox peak current values increase linearly. Meanwhile it can be clearly seen from **Fig. 1E** that as the scan rate increases, the peak current of the anode (red line) increases, while the peak current of the cathode (black line) decreases. This proves that the polymerized FMMA is covalently bound to the heteroduplex of PNA/ T-DNA.[33]

Through electrochemical impedance spectroscopy (EIS) , which has high sensitivity for detecting the slight differences between solid-liquid interfaces, the process of electrode surface stepwise modification was characterized to further verify the reliability of this strategy. As shown in **Fig. 1F**, EIS can be equivalent to an equivalent circuit composed of the electrolyte solution resistance R_s, the surface electron transfer resistance R_{ct} and the Warburg impedance Z_w through series and parallel. **Fig. 1F** shows the Nyquist curve of the stepwise modification process, the charge transfer dynamics of $[Fe(CN)_6]^{3-/4-}$ are reflected in R_{ct} which corresponds to the diameter of the semi-circular arc in the high frequency. As shown in **Fig. 1F**, the bare gold electrode shows an extremely small semicircular arc (R_{ct} = 103.9 Ω, **curve a**), which indicates that the charge $[Fe(CN)_6]^{3-/4-}$ transfers very quickly on the surface of gold electrode. However, due to steric hindrance, when PNA (R_{ct} = 1313.6 Ω, **curve b**) and MCH (R_{ct} = 2028.7 Ω, **curve c**) are gradually fixed to the electrode surface, the self-assembled monolayer (SAM) formed hinders charge transfer, It can be seen that the impedance value gradually increases. Subsequently, due to the mutual repulsion between the negatively charged $[Fe(CN)_6]^{3-/4-}$ and phosphate, when T-DNA is hybridized with PNA, it can be observed that the semicircular arc significantly increases (R_{ct} = 2834.8 Ω, **curve d**). Then, when Zr^{4+} was connected with PNA/ T-DNA heteroduplex, we observed an interesting phenomenon, R_{ct} further increased (R_{ct} = 3589.4 Ω, **curve e**). This is because Zr^{4+} adsorbs $[Fe(CN)_6]^{3-/4-}$ to the surface of the gold electrode through electrostatic attraction, which causes electrostatic repulsion to the charge transfer on the electrode surface. Subsequently, when the initiator BPAA and the catalyst MnTBAP of ATRP were combined with the vacant sites of Zr^{4+}, the steric hindrance of the electrode surface changed and the hydrophilicity decreased significantly, resulting in $[Fe(CN)_6]^{3-/4-}$ not easily to transfer on the electrode surface, and R_{ct} continues to increase (R_{ct} = 4304.6 Ω, **curve f**). Finally, when a large number of FMMA monomers are polymerized onto the PNA/ T-DNA heteroduplex via ATRP, due to the formation of the polymer, the transmission of charges on the electrode surface is spatially hindered, and a large circular arc (**curve g**) with a large R_{ct} value of about 6034.8 Ω can be seen. These results further confirm the successful fabrication of the DNA biosensor according to **Scheme 1A**.

In addition, in order to better illustrate the feasibility of ATRP. The surface of the electrode before and after ATRP was analyzed by X-ray photoelectron spectroscopy (XPS). **Fig. S1** shows the Fe 2p energy level spectrum of XPS. Before ATRP, the presence of Fe element was not observed. However, after ATRP, we can clearly see the XPS peak of Fe. It is a good proof that the ATRP reaction has been successfully applied to electrochemical DNA biosensors.

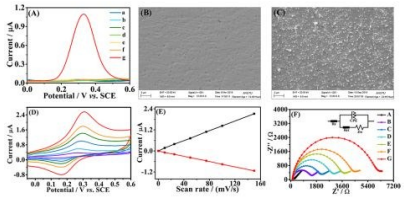

Fig. 1 (A) Square wave voltammogram corresponding to gold electrode (g) modified with PNA/ MCH/ T-DNA/ Zr^{4+}/ BPAA-MnTBAP/ $FMMA_n$ and the SWV corresponding to PNA (a), T-DNA (b), Zr^{4+} (c), BPAA (d), MnTBAP (e) or FMMA (f) were not added in the process of electrode surface modification. **(B)**, **(C)** The SEM images of a fully modified electrode **(C)** and no T-DNA was added during electrode surface modification **(B)**. **(D)** CV of a fully modified gold electrode in 0.5M $LiClO_4$ solution, with scan speeds of 0, 10, 25, 50, 75, 100, and 150 mV s^{-1}, respectively. **(E)** The linear relationship between the peak current of the anode (black line) and cathode (red line) and the scan rate in Fig. 1D. **(F)** Nyquist curves of electrodes at different modification stages. (A) Bare electrodes, (B) PNA, (C) PNA/ MCH, (D) PNA/ MCH/ T-DNA, (E) PNA/ MCH/ T-DNA/ Zr^{4+}, (F) PNA/ MCH/ T-DNA/ Zr^{4+}/ BPAA-MnTBAP, (G) PNA/ MCH/ T-DNA/ Zr^{4+}/ BPAA-MnTBAP/ $FMMA_n$.

View Article Online
DOI: 10.1039/D0CC02176H

Then, in order to obtain higher sensitivity, we optimized the experimental conditions such as the hybridization time of the PNA/DNA heteroduplex and the polymerization time of ATRP. In order to make the analysis process more convenient and efficient, and to perform DNA detection quickly, many experimental conditions need to be optimized. First, we optimized the time for PNA to bind to DNA. **Fig. S2A** shows the optimization of PNA/DNA heteroduplex binding time. From the **Fig. S2A**, we can see that after 90 minutes of binding, the electrochemical signal gradually stabilizes, indicating that PNA and DNA can be well combined at 90 minutes. Therefore, we chose 90 minutes as the optimal binding time between PNA and DNA. In addition, in order to further accelerate the experimental process and shorten the time required for ATRP reaction, we optimized the time of ATRP reaction. As shown in **Fig. S2B**, when the reaction time is about 90 minutes, the detected signal value of ferrocene reaches the maximum, and then the signal rise is very small. With the extension of ATRP reaction time, the efficiency of the polymerization reaction decreased significantly. On the one hand, it may be the radical-free radical termination reaction being significantly intensified; on the other hand, it may also be due to the large number of chain-proliferating free radicals being embedded in the polymer by the growing polymer chain, so that the monomer cannot continue to the polymerization reaction. Therefore, considering the enrichment amount of electroactive substances and analysis time, a 90 minutes ATRP reaction time was used in subsequent experiments.

To analyze the performance of the proposed electrochemical DNA biosensor, the prepared electrode was subjected to SWV analysis in $LiClO_4$ solution under optimal conditions. It can be seen from **Fig. 2A** that an obvious oxidation appears at ~0.33V, and the peak value of oxidation current increases with the increase of T-DNA concentration in the range of 100 aM-100 pM. At the same time, the oxidation peak at the potential of ~0.33V is consistent with the position of the FMMA peak reported in the literature. In addition, after processing, it can be seen that the logarithm of the target DNA concentration in the range of 100 aM-100 pM and the peak value of the oxidation current show a good linear relationship (**Fig. 2B**). Through calculation, the linear regression equation is: $I= 0.14\log C_{T\text{-}DNA/\ aM} -0.1$ (R^2 = 0.997). The detection limit is 11.79 aM. It means that in a 10 μL sample, 71 copies can be detected. The detection limit of this method is far lower than that reported so far (as shown in **Table S2**). On the one hand, because this method uses PNA as a capture probe, there is no phosphate group such as DNA and ribonucleic acid (RNA), so the lack of electrical repulsion between PNA and DNA, which makes the binding strength between PNA and DNA stronger than that between DNA and DNA, thus greatly enhancing the capture performance of the sensor.[34,35] On the other hand, due to the ATRP signal amplification reaction catalyzed by MnTBAP, a large amount of polymers formed by the electroactive probes are introduced on the electrode surface, which can significantly improve the sensitivity of electrochemical detection. Therefore, this method can be used in the electrochemical high-sensitivity biosensor analysis of DNA, and has great market application prospects.

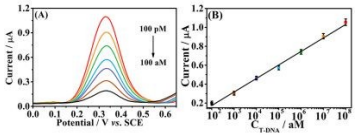

Fig. 2 (A) Correspondence between SWV and T-DNA at different concentrations in the range of 100 aM to 100 pM. (B) A plot of the linear relationship between the logarithm

of T-DNA concentration and the oxidation peak current. Error bars correspond to the standard deviation of 6 replicate experiments.

To explore the selectivity of this protocol, the oxidation peak currents of 100 fM T-DNA, single base mismatch DNA (SM-DNA), three-base mismatch DNA (TM-DNA), non-complementary DNA (N-DNA), and blank control (Control) were analyzed via square wave voltammetry (SWV). It can be calculated from **Fig. 3A** that the oxidation peak current values detected by SM-DNA and TM-DNA are only 24.27% and 15.91% of T-DNA. The results demonstrate that the proposed electrochemical DNA biosensor has good selectivity and can clearly distinguish single-base misaligned sequences. In addition, N-DNA and blank controls have almost no electrochemical response, further indicating that the sensor can distinguish DNA fragments of different sequences. This is due to the fact that PNA is neither a polypeptide nor a nucleic acid. Therefore, PNA is not easily hydrolyzed by proteases or nucleases. PNA is quite stable in vivo and in vitro. At the same time, due to the strong specificity of base pairing, PNA has high thermal stability. On the other hand, due to the successful preparation of the ATRP signal amplification strategy. Therefore, the ATRP electrochemical biosensor catalyzed by MnTBAP with PNA as a capture probe is suitable for detection and analysis of single nucleotide polymorphisms (SNPs). In addition, the reproducibility and stability of the DNA biosensor have also been studied. The reproducibility was analyzed using inter-assay and intra-assay test results. The coefficients of variation between batches and within batches were 4.62% and 4.05%, indicating that it has reliable repeatability. At the same time, we also investigated the stability of the electrochemical DNA biosensor. The sensor was stored at 4 °C for one month, and the recovery rate of SWV response could reach 96.85%, and the results showed satisfactory stability.

In order to evaluate the universality and anti-interference ability of the DNA electrochemical biosensor in complex biological sample analysis. Different concentrations of T-DNA (100 pM, 100 fM, 100 aM) were added to phosphate buffer saline (PBS), 1% (v/v) diluted healthy human serum (NHS) and 10% (v/v) NHS respectively, and mixed evenly, and the above samples were detected with this sensor. The electrochemical response signal recovery of 100pM, 100fM and 100aM T-DNA in 1% NHS were 97.81%, 94.62% and 88.39%, respectively. And in 10% NHS, the recoveries of 100pM, 100fM and 100aM T-DNA were 93.18%, 87.82% and 80.85%, respectively (**Fig. 3B**). The results show that the detection of the DNA electrochemical biosensor is feasible in actual biological samples.

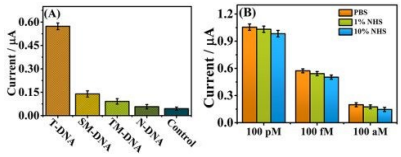

Fig. 3 (A) The signal amplification method is used for the oxidation peak current value of ~0.33V vs. SCE for electrochemical biosensor analysis of different DNA (T-DNA, SM-DNA, TM-DNA, N-DNA) and a blank control. The concentration of these samples was 0.1 pM. (B) Oxidation current peaks at ~0.33V vs. SCE at different concentrations of T-DNA in 0.1 M PBS (pH 7.6), 1% NHS and 10% NHS. The error bar corresponds to the standard deviation of 6 replicate experiments.

In conclusion, using PNA as the immobilized capture probe, and with the help of ATRP catalyzed by MnTBAP to polymerize FMMA directly onto the captured T-DNA as an electroactive probe, a simple electrochemical method was established. It enables the analysis of DNA with high selectivity, high sensitivity, high throughput and environment protecting. Using PNA as a capture probe to specifically recognize T-DNA significantly improves the selectivity of DNA biosensor, which can effectively distinguish base misplaced DNA, so it is suitable for SNPs analysis. Under the optimal conditions, the method can be used for rapid analysis of T-DNA in the range of 100 aM-100 pM (R^2 = 0.997), and the detection limit is 11.79 aM. Moreover, the method has universality and strong anti-interference ability in the analysis of complex biological samples. Therefore, the ATRP signal amplification strategy based on MnTBAP can not only provide excellent signal response when detect various tumor markers (such as RNA and protein), but also can be easily performed at room temperature with high throughput and can be carried out under the green conditions.

We thank the National Natural Science Foundation of China (Grant No. 21974068) for support.

Conflicts of interest

There are no conflicts of interest to declare.

Notes and References

1. M. Soler, M. C. Estevez, R. Villar-Vazquez, J. I. Casal and L. M. Lechuga, *Anal. Chim. Acta*, 2016, **930**, 31-38.
2. J. Phallen, M. Sausen, V. Adleff, A. Leal, C. Hruban, J. White and S. Speir, *Sci. Transl. Med*, 2017, **9**, 403.
3. A. M. Aravanis, M. Lee and R. D. Klausner, *Cell*, 2017, **168**, 571-574.
4. S. Liu, C. Wang, C. Zhang, Y. Wang and B. Tang, *Anal. Chem*, 2013, **85**, 2282-2288.
5. I. Grabowska, D. G. Singleton, A. Stachyra, A. Góra Sochacka,A. Sirko, W. Zagórski Ostoja, H. Radecka, E. Stulz and J. Radecki, *Chem. Commun*, 2014, **50**, 4196-4199.
6. Y. Qian, C. Wang and F. Gao, *Biosens. Bioelectron*, 2015, **63**, 425-431.
7. Y. H. Liu, H. N. Li, W. Chen, A. L. Liu, X. H. Lin and Y. Z. Chen, *Anal. Chem*, 2012, 85, 273-277.
8. G. Liu, Y. Wan, V. Gau, J. Zhang, L. Wang, S. Song and C. Fan, *J. Am. Chem. Soc*, 2008, **130**, 6820-6825.
9. J. A. Hansen, R. Mukhopadhyay, J. Ø. Hansen and K. V. Gothelf, *J. Am. Chem. Soc*, 2006, **128**, 3860-3861
10. A. Sassolas, B. D. Leca-Bouvier and L. J. Blum, *Chem. Rev*, 2008, **108**, 109-139.
11. W. Gao, H. Dong, J. Lei, H. Ji and H. Ju. *Chem. Commun*, 2011, **47**, 5220-5222.
12. P. Fanjul-Bolado, D. Hernández-Santos, M. B. González-García and A. Costa-García, *Anal. Chem*, 2007, **79**, 5272-5277.
13. K. Hsieh, Y. Xiao and H. T. Soh. *Langmuir*, 2010, **26**, 10392-10396.
14. P. Ling, J. Lei and H. Ju, *Biosens. Bioelectron*, 2015, **71**, 373-379.
15. G. Wu, N. Yang, T. Zhang, Z. Wang, X. Lu and J. Kang, *Sensor. Actuat. B-Chem*, 2011, **160**, 598-603.
16. S. Liu, P. Wu, W. Li, H. Zhang and C. Cai, *Anal. Chem*, 2011, **83**, 4752-4758.
17. G. Nallur, C. Luo, L. Fang, S. Cooley, V. Dave, J. Lambert, K. Kukanskis, S. Kingsmore, R. Lasken and B. Schweitzer, *Nucleic. Acids. Res*, 2001, **29**, e118-e118.
18. W. Zhao, M. M. Ali, M. A. Brook and Y. Li, *Angew. Chem. Int. Edit*, 2008, **47**, 6330-6337.
19. M. M. Ali, F. Li, Z. Zhang, K. Zhang, D. K. Kang, J. A. Ankrum, X. C. Le and W. Zhao, *Chem. Soc. Rev*, 2014, **43**, 3324-3341.
20. P. Harding Lepage, R. Peytavi, M. G. Bergeron and M. Leclerc, *Anal. Chem*, 2011, **83**, 8086-8092.
21. H. Liu, D. Wang, Z. Song, and S. Shang, *Cellulose*, 2011, **18**, 67-74.
22. J. M. Gibbs, S. J. Park, D. R. Anderson, K. J. Watson, C. A. Mirkin and S. T. Nguyen, *J. Am. Chem. Soc*, 2005, **127**, 1170-1178.
23. H. Tan, S. Yang, G. Shen, R. Yu and Z. Wu, *Angew. Chem. Int. Edit*, 2010, **122**, 8790-8793
24. H. Sun, Y. Qiu, Q. Liu, Q. Wang, Y. Huang, D. Wen, J. Kong, *Biosens. Bioelectron*, 2019, **131**, 193-199.
25. J. S. Wang and K. Matyjaszewski, *Macromolecules*, 1995, **28**, 7901-7910.
26. J. S. Wang and K. Matyjaszewski, *J. Am. Chem. Soc*, 1995, **117**, 5614-5615.
27. H. Sun, J. Kong, Q. Wang, Q. Liu and X. Zhang, *ACS. Appl. Mater. Inter*, 2019, **11**, 27568-27573.
28. B. Liu, H. Sun, L. Li, J. Zhang, J. Kong and X. Zhang, *Microchim. Acta*, 2020, **187**, 35.
29. C. M. Che and J. S. Huang, *Chem. Commun*, 2009, **27**, 3996-4015.
30. T. Wang, Y. She, H. Fu and H. Li, *Catal. Today*, 2016, **264**, 185-190
31. M. G. de Araujo Tôrres, V. S. da Silva, Y. M. Idemori and G. DeFreitas-Silva, *Arab. J. Chem*, 2020, **13**, 1563-1574.
32. M. J. Shiddiky, A. A. Torriero, Z. Zeng, L. Spiccia and A. M. Bond, *J. Am. Chem. Soc*, 2010, **132**, 10053-10063.
33. H. Chang, L. Tang, Y. Wang, J. Jiang and J. Li, *Anal. Chem*, 2010, **82**, 2341-2346.
34. J. Zhang, B. P. Ting, N. R. Jana, Z. Gao and J. Y. Ying, Small, 2009, **5**, 1414-1417.
35. Y. Fan, X. Chen, J. Kong, C. H. Tung and Z. Gao, *Angew. Chem. Int. Edit*, 2007, **46**, 2051-2054.